International Journal of Robotics and Control Systems
Vol. 5, No. 2, 2025, pp. 1156-1171
ISSN 2775-2658
http://pubs2.ascee.org/index.php/ijrcs

Strategic Chess Algorithm-Based PI Controller Optimization for Load Frequency Control in Two-Area Hybrid Photovoltaic–Thermal Power Systems

Jagraphon Obma [a,1], Sitthisak Audomsi [b,2], Kittipong Ardhan [c,3] , Worawat Sa-Ngiamvibool [b,d,4], Natpapha Chansom [e,5,*]

[a] Department of Computer Engineering, Rajamangala University of Technology ISAN, Khonkaen Campus, Khonkaen, Thailand
[b] Faculty of Engineering, Mahasarakham University, Maha Sarakham, 44150, Thailand
[c] Faculty of Engineering and Industrial Technology, Kalasin University, Karasin province, 46000, Thailand
[d] Electrical and Computer Engineering Research Unit, Mahasarakham University, Mahasarakham 44150, Thailand
[e] Department of Mechatronics Engineering, Rajamangala University of Technology ISAN, Khonkaen Campus, Khonkaen, Thailand
[1] Jagraphon.ob@rmuti.ac.th; [2] 67010361003@msu.ac.th; [3] Kittipong.ar@ksu.ac.th; [4] Wor.nui@gmail.com;
[5] Natpapha.ch@rmuti.ac.th
* Corresponding Author

ARTICLE INFO

Article history
Received March 22, 2025
Revised April 26, 2025
Accepted May 01, 2025

Keywords
Load Frequency Control;
Chess Algorithm Optimization;
Hybrid Photovoltaic–Thermal Systems;
PI Controller Tuning;
Frequency Regulation in Renewable Grids

ABSTRACT

Maintaining frequency stability in hybrid renewable-integrated power systems remains a critical challenge due to the inherent variability and uncertainty of photovoltaic–thermal (PV–T) energy sources. Traditional proportional–integral (PI) controllers, optimized using conventional metaheuristic algorithms such as the Whale Optimization Algorithm (WOA), Firefly Algorithm (FA), and Salp Swarm Algorithm (SSA), often suffer from limitations including slow convergence, premature convergence to local optima, and reduced robustness under severe load disturbances. The research contribution is the development and systematic evaluation of a chess algorithm (CA)-based PI controller tuning approach for enhancing load frequency control (LFC) in hybrid PV–T systems. Unlike population-based methods, the CA employs chess-inspired strategic decision-making processes, which improve the search efficiency and the ability to escape local optima in high-dimensional optimization problems. In this study, the proposed CA-based optimization method is applied to a two-area hybrid PV–T power system, where the system is subject to various operating conditions, including solar radiation fluctuations and step load perturbations. The tuning of PI controller parameters is performed using the integral of time-weighted absolute error (ITAE) as the objective function. Simulation results demonstrate that the CA-optimized PI controller achieves superior performance in minimizing overshoot, undershoot, and settling time when compared with controllers optimized by WOA, FA, and SSA. Specifically, the CA approach achieves faster stabilization and lower frequency deviations, highlighting its potential for real-time implementation and enhanced grid reliability. Future work will explore the scalability of the proposed method to multi-area power systems and evaluate its computational efficiency through hardware-in-the-loop validation.

1. Introduction

The growing adoption of renewable energy sources (RESs) [1], [2] and [3], particularly photovoltaic (PV) systems, has profoundly altered the operating dynamics of contemporary power systems [4]. Although these systems have environmental and economic advantages, their sporadic and unexpected characteristics provide significant issues for sustaining power system stability, particularly in frequency management. Photovoltaic–thermal (PV–T) hybrid systems, integrating solar photovoltaic generation with thermal power sources, are being utilized to enhance energy efficiency. The intrinsic unpredictability of solar irradiance and the erratic nature of renewable output can result in significant frequency variations, jeopardizing the stability and dependability of power networks [5].

Load Frequency Control (LFC) systems are usually used to solve these difficulties by keeping the real-time balance between power generation and consumption [6], [7] and [8]. Conventional LFC approaches typically use proportional–integral (PI) [9] or proportional–integral–derivative (PID) controllers [10], [11] to regulate power output in response to frequency deviations. But in hybrid renewable systems, where system dynamics are extremely nonlinear and prone to great uncertainty, the tuning of PI/PID controllers is progressively more difficult [12], [13] and [14].

Recent studies have investigated a range of optimization techniques aimed at improving the performance of PI/PID controllers in LFC applications [15], [16] and [17]. Among these, the Whale Optimization Algorithm (WOA) [18], [19] and [20], Firefly Algorithm (FA) [21], [22] and Salp Swarm Algorithm (SSA) [23], [24] and [25] have demonstrated considerable potential. Nonetheless, these algorithms continue to demonstrate significant limitations, such as premature convergence, an inadequate balance between exploration and exploitation, and a sluggish convergence speed in high-dimensional search environments. The identified shortcomings impede their effectiveness in highly dynamic systems, such as hybrid PV–T power grids [26], [27] and [28].

To overcome these challenges, this study proposes the use of the Chess Algorithm (CA) [29], [30] a novel metaheuristic optimization method inspired by the strategic decision-making processes of chess gameplay. Unlike traditional swarm-based or population-based algorithms, CA employs piece-specific strategies, prioritizing certain solution candidates based on tactical movements akin to those used in chess. This characteristic enhances its ability to explore the search space effectively, avoid local optima, and achieve faster convergence.

The research contribution is the development and systematic evaluation of a chess algorithm-based PI controller tuning approach for load frequency control in two-area hybrid photovoltaic–thermal power systems. This study specifically investigates whether the strategic optimization process of CA can address the recognized deficiencies of existing metaheuristic methods in controller tuning, thereby improving frequency regulation performance under varying load disturbances and solar radiation conditions.

The remainder of this paper is structured as follows: Section 2 describes the modeling of the two-area hybrid PV–T power system and the formulation of the chess algorithm-based optimization framework. Section 3 presents the simulation setup and parameters. Section 3.1 discusses the results, comparing the performance of CA with WOA, FA, and SSA. Section 4 concludes the study and outlines directions for future research.

2. Methodology

2.1. Two-Area Power System

In Fig. 1, our basic model of the work is a two-area test system, shown as follows: The two-system independent zones represent a mixed power grid of thermal production sources and photovoltaic (PV) technologies synthesis. Zone 1 is PS: photovoltaic system with maximum power point tracking (MPPT) [31], [32] and [33]. As you can see, the MPPT system that powers solar panels extracts the maximum energy as always. This system will follow the changes in solar radiation,

Vol. 5, No. 2, 2025, pp. 1156-1171

ambient temperature, and many more external conditions that the panels face from the MPPT system. In the second zone of the system, a reheat thermal unit that makes electricity by conventional means (usually nuclear or fossil fuels) is placed to produce steam [34].

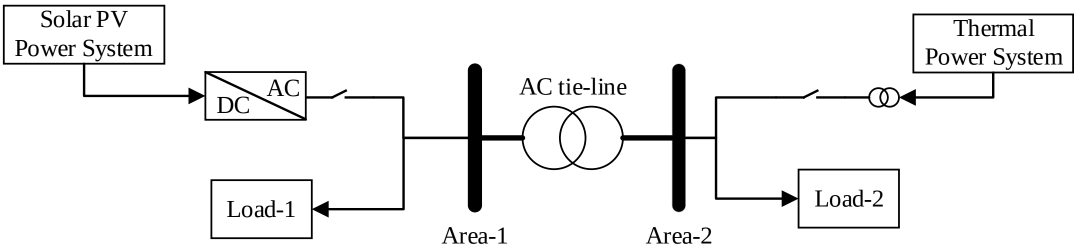

Fig. 1. Schematic representation of the power system, adapted from [35]

Fig. 2 illustrates the use of MATLAB/Simulink tools to replicate and model each component of the testing system, including their interrelationships. This environment aided in the construction of high-fidelity models for every component, ranging from the PV array to the governor mechanism [36], turbine assembly, reheater module and the entire power system. Appropriate transfer functions for each component to illustrate the description of the structure state movement. First-Order Linear Approximations of transfer functions help mathematical analysis because they show how system parts interact [37], [38] and [39].

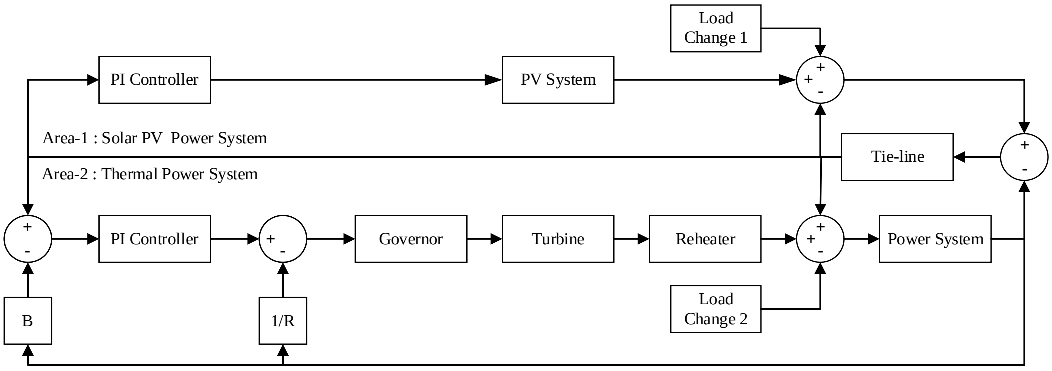

Fig. 2. Two-area power system under study, adapted from [40]

Equations 1–5 describe the mathematical representations of the building blocks, which are the PV system and the thermal unit, and their transfer functions relative to each other and their interactions within the broader dynamics of the system. The MPPT algorithm is implemented within the PV system model for the system [41] (so that it literally turns itself into a hotter, more efficient, lighter energy harvester that dynamically senses high-quality sunshine and gathers maximum energy from PV panels regardless of the continuously changing weather [42]. This means that the system will react in an ideal fashion with regard to efficiency under any environmental condition.

However, for that PV system to work in MPPT mode [43], it must always produce energy and power at its highest level. If it doesn't, it won't be able to adapt to changes in the system frequency at a low level. [MPPT mode needs to blow the whistle for energy generation, competing with little or no trait of frequency management.] However, there is no frequency coming back from the photovoltaic panels in Area 1. This limitation suggests that the photovoltaic system [44], while effective for energy production, does not aid in frequency shedding under standard operating conditions. The fact that the photovoltaic system couldn't control the frequency showed a problem: adding photovoltaic power to a grid can cause stability problems. This is especially true as more renewable energy systems are added.

The transfer function of the PV system is defined by Equation (1), illustrating its composite structure derived from several components [32].

$$G_{PV} = \frac{-As + E}{s^2 + C_T s + D_T} \tag{1}$$

This expression describes the time-variant behavior of PV system, highlighting its sensitivity to solar irradiance and temperatures changes. The transfer function will allow broad time variation of system in varying environmental conditions.

- System dynamics: The inclusion of $s^2 + C_T s + D_T$ in the denominator says that there is some sort of dependency for power output and how responsive you are to changes in environmental parameters. The constants control the speed and stability of system reaction, C_T and D_T .
- Response control: Numerator constants A and E control the responsivity and output of the PV system. Changing these constants could increase the ability of the system to respond quickly to changes in solar irradiation and temperature.

The transfer function of the governor system is defined by Equation (2), illustrating its composite structure derived from several components [45], [46] and [47].

$$G_{GVR} = \frac{K_G}{1+ s\tau_G} \tag{2}$$

Where G_{GVR} this shows the governor's reaction to changes in system frequency and its modulation of the power output of the generator. To keep the grid stable, the governor guarantees the generator runs at a recommended power level. K_G expresses the governor's gain constant. It shows the extent to which the governor responds to frequency changes by varying the output of the generator. An elevated K_G denotes that in response to a given frequency fluctuation the governor will implement a more significant change to the generator's output. τ_G The governor's time constant is shown here. It indicates the time the governor needs to react to a frequency modification. Whereas an increased τ_G denotes a more lethargic response, a reduced τ_G indicates a faster reaction. The governor's inertia or the period required for the system to adjust to changes is indicated by the time constant [48].

Equation (3) defines the turbine's transfer function, therefore defining the dynamic reaction of the turbine in converting mechanical work from its input. One writes the transfer function as:

$$G_{TRB}= \frac{K_T}{1+ s\tau_R} \tag{3}$$

Where G_{TRB} is the transfer function of the turbine, it mathematically expresses the turbine response to changes in the input, for example frequency changes in the power system. It also provides insight into how quickly and efficiently the turbine converts energy from the generator to mechanical work. K_T The turbine gain constant [49], which relates to the turbine's ability to convert energy from eigenoperator into mechanical work. It defines the amount of output power that turbine produces for a given input signal. τ_R, which is the time constant of the turbine in seconds, determines how rapidly the turbine can respond to changes in its input. A bigger τ_R translates into slower, thus a slower reacting turbine which will take longer to respond to frequency disturbances in the power system. Larger τ_R means a slower turbine response [50].

Equation (4) delineates the transfer function of the reheater, G_{RHT} , inside a power system. The text delineates the dynamic behavior of the reheater, which is tasked with regulating the temperature of steam in thermal power systems, primarily to optimize power generating efficiency. The formula is:

$$G_{RHT} = \frac{1 + sK_R\tau_R}{1 + s\tau_R} \tag{4}$$

The power system's transfer function is given by following Equation (5):

$$G_{PS} = \frac{K_{PS}}{1 + s\tau_{PS}} \tag{5}$$

Where G_{PS} represents the transfer function of the power system. It simulates the dynamic response of the entire power system to fluctuations, including frequency variations or load alterations. K_{PS}: This is the gain constant of the power system, indicating the system's general responsiveness to variations in input, such as power consumption or fluctuations in system frequency. A greater K_{PS} signifies that the system exhibits a more robust response to stimuli. τ_{PS}: This is the time constant of the power system, signifying the speed at which the system responds to input variations. A bigger τ_{PS} signifies a slower system response, whereas a smaller τ_{PS} denotes a quicker reaction.

2.2. Chess Algorithm

The Chess Algorithm (CA) is a metaheuristic optimization technique that draws inspiration from the strategic decision-making and maneuvering exhibited by chess players throughout a game [30]. This algorithm tackles intricate optimization challenges by emulating the strategic reasoning and adaptive maneuvers found in chess, where each piece functions with distinct roles and movement patterns. In contrast to traditional population-based optimization methods, CA utilizes chess-specific strategies, including pawn deployment for exploration and prioritization of pieces (king, queen, rooks, bishops, and knights) for exploitation. This approach facilitates a balanced search behavior in high-dimensional and nonlinear search spaces [51], [52] and [53].

The chess algorithm's optimization process encompasses several essential steps: initialization, evaluation, strategic arrangement of chess pieces, local search refinement, and the selection of optimal solutions. The steps are systematically repeated until the convergence criteria are satisfied, which may include attaining the minimum objective function value or reaching the maximum allowable number of iterations [54], [55] and [56].

The overall flow of the chess algorithm-based optimization applied in this research is illustrated in Fig. 3, which presents the systematic sequence of operations for controller parameter tuning using CA.

2.3. Load Frequency Control Utilizing Chess Algorithms

The most likely scenario is that this component of the power system will have frequency variations due to power generation and consumption imbalances. There can be a load demand that exceeds production or does not produce enough to meet the required loads, and then the frequency of the system may either rise or fall. Some causes of this disparity include variations in renewable energy sources, such as the sun and wind, abrupt changes in demand, or generator malfunction. Therefore, this needs to be followed and corrected for stability. One primary tool for this is known as the Area Control Error (ACE) [57].

In a multi-area power system, the ACE signals of Area-1 and Area-2 are computed individually to function jointly for the total stability of the entire system. The ACE signals from both the areas can be represented as follows Equation (6), (7):

- Area-1:

$$ACE_1 = B_1 \cdot \Delta f_1 + \Delta P_{tie,1} \tag{6}$$

- Area-2:

$$ACE_2 = B_2 \cdot \Delta f_2 + \Delta P_{tie,2} \tag{7}$$

Where Δf_1 and Δf_2 are the frequency deviations for Area-1 and Area-2, respectively. B_1 and B_2 are the frequency bias parameters for Areas 1 and 2, respectively. $\Delta P_{tie,1}$ and $\Delta P_{tie,2}$ represents the power discrepancies on the interconnections between Area-1 and Area-2 [58]. The ACE signal is crucial for maintaining the stability and efficiency of power networks by consistently detecting differences between power output and demand. The LFC controller employs the ACE signal as its primary input to regulate power generation in real-time, hence preserving system stability and optimal operational conditions. The LFC system alleviates substantial frequency variations, hence improving the reliability and efficiency of the power grid.

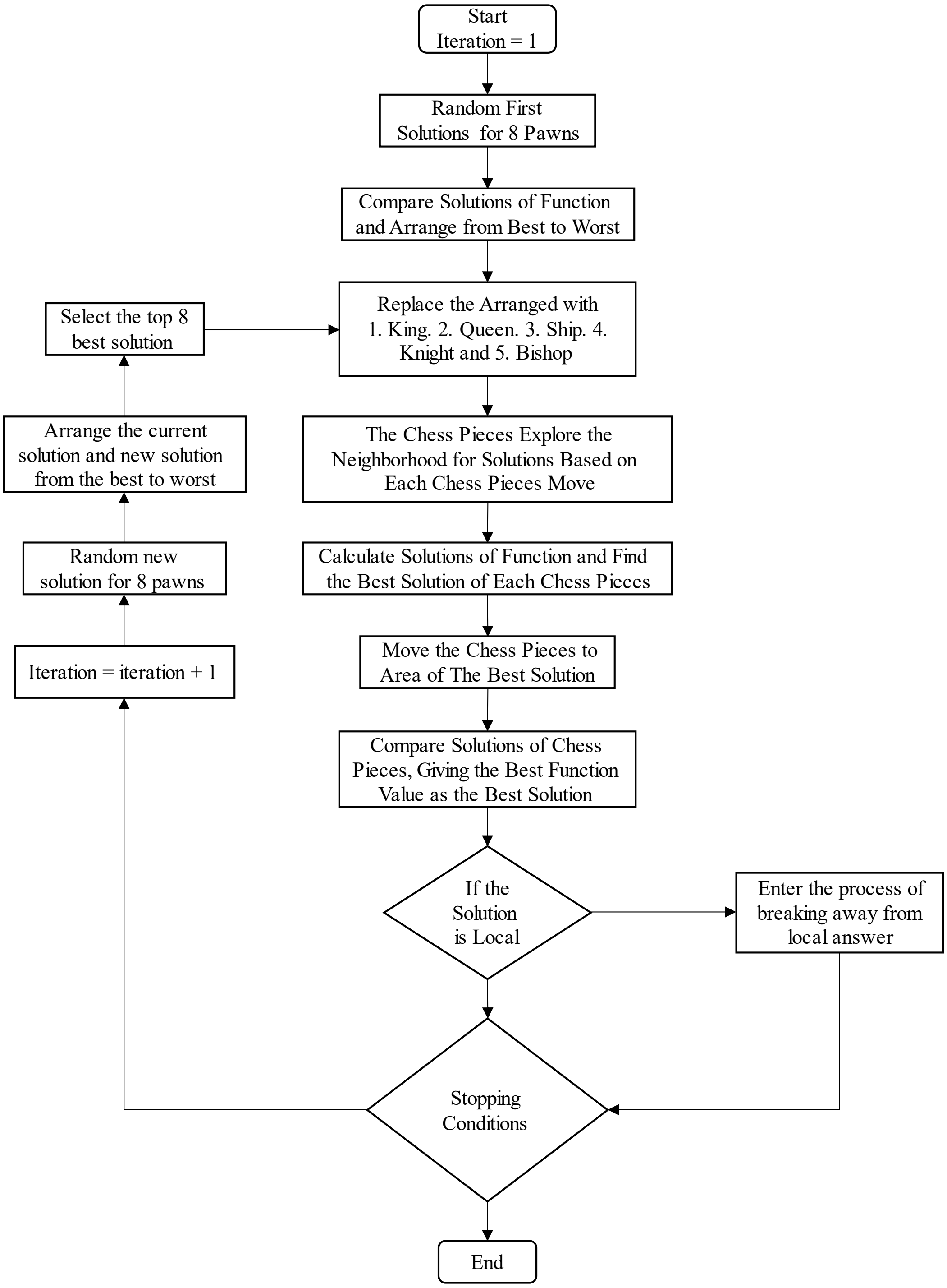

Fig. 3. Flowchart of chess optimization algorithm

2.4. Controller Structure and Parameter Constraints

A PI (Proportional-Integral) Controller is a widely utilized control mechanism in various systems, including Load Frequency Control (LFC) for power systems. The PI controller combines two control actions: proportional and integral, with the objective of reducing errors and stabilizing the system by adjusting the output in response to deviations from a setpoint [59]. The transfer function of a PI controller can be expressed as Equation (8):

$$G_{PI}(s) = K_p + \frac{K_i}{s} \tag{8}$$

Where K_p is the proportional gain and K_i is the integral gain. This research will utilize CA optimization based on the controller gains for optimization. The main goal function changes to the ITAE integral goal, which looks at the differences in frequency between the two areas and the changing tie-line power. The following ITAE criterion objectified in Equation (9) will determine the ideal controller gains for improved power system performance [60]. ITAE will serve as a performance measure. This criterion paves the way toward the optimization of a controller for quick response yet stable performance. ITAE calculates the integrated product of the controller and the error at a specific time in the ACE signal, thus a controller performance benchmarking. For all load frequency control, the use of the ITAE performance index is vital considering its merits toward penalizing steady-state error through time. Such priority is crucial in power systems because prolonged excursions cause inefficiency and instability throughout the network. Therefore, by making controller gains minimum in ITAE, we aim to increase the resilience and sensitivity of the system against frequency disturbances that would lead to quicker adjustments in setpoints and eventually a better stable condition [60].

$$ITAE = \int_0^{30} t\left(|\Delta f_i| + |\Delta P_{tie}|\right) dt \tag{9}$$

Where Δf_i denotes the frequency deviations for Area i, t signifies the time simulation and ΔP_{tie} indicates the power disparities on the interconnections between Area-1 and Area-2.

In the optimization of PI controllers, the gain parameters K_p (Proportional gain) and K_i (Integral gain) must be restricted between specified lower and higher limits. These limits are crucial as they delineate the permissible values for the controller's gains, guaranteeing that the system operates reliably and effectively throughout diverse operating situations. The optimization method seeks to identify the optimal combination of K_p and K_i that reduces error or increases system performance, while adhering to limitations to prevent instability, overshoot, or unpleasant oscillations. The limits for the gains of the PI controller, K_p and K_i are defined by the subsequent equations, referred to as Equation (10) and Equation (11). These equations delineate the permissible range for each gain parameter.

$$K_{p\,min} \le K_p \le K_{p\,max} \tag{10}$$

$$K_{i\,min} \le K_i \le K_{i\,max} \tag{11}$$

The suggested CA method seeks to enhance the gain parameters of a PI controller by employing the ITAE objective function as delineated in Equation (9) and accounting for the variable restrictions specified in Equations (10) and (11). as seen by the arrangement shown in Fig. 2. For more information concerning the parameter parameters of the test model, please see Table 1. The parameters of the proposed CA algorithm are detailed in Table 2, along with the block design of the PI controller for the LFC issue.

To ensure a fair and unbiased review of performance, the suggested Chess Algorithm (CA)-based optimization method is compared with three well-known metaheuristic algorithms: the Whale Optimization Algorithm (WOA), the Firefly Algorithm (FA), and the Salp Swarm Algorithm (SSA). All optimization approaches are executed under identical simulation conditions to ensure consistency and reproducibility of the results. Specifically, the number of iterations for each algorithm is set to 50, and the proportional–integral (PI) controller gain parameters are constrained within the bounds of [−2, 2]. The settings for WOA, FA, and SSA are taken from proven configurations found in earlier research, ensuring a trustworthy way to compare and fairly evaluate their optimization performance.

Table 1. Test system parameter [61]

Parameters	Full name of parameters	Value	Unit
A	Photovoltaic System Gain 1	18	-
E	Photovoltaic System Gain 2	900	-
C_T	Photovoltaic system time constant 1	100	-
D_T	Photovoltaic system time constant 2	50	-
K_G	Governor gain	1	p.u.MW
τ_G	Governor time constant	0.08	sec
K_T	Turbine gain	1	p.u.MW
τ_T	Turbine time constant	0.3	Sec
K_R	Reheat gain	0.33	p.u.MW
τ_R	Reheat time constant	10	sec
K_{PS}	Power system gain of thermal area	120	Hz/p.u.MW
τ_{PS}	Power system time constant	20	sec
R	Regulation droop	0.4	Hz/p.u.MW
B	Frequency bias constant	0.8	p.u.
τ_{tie}	Tie-line power coefficient	0.545	-

Table 2. Comparative comparison of parameters for CA, WOA [62], FA [63], and SSA [35] in addressing the LFC problem

Parameter	CA (Proposed)	WOA	FA	SSA
Iteration number	50	50	50	50
Lower bound for PI	[-2; -2]	[-2; -2]	[-2; -2]	[-2; -2]
Upper bound for PI	[2; 2]	[2; 2]	[2; 2]	[2; 2]
Contrast of the attractiveness	-	-	1.0	-
Attractiveness at r = 0	-	-	0.1	-
Randomization parameter ($\propto$)	-	-	0.1	-
Mutation probabilities	-	0.4	-	-
Rate of procreation	-	0.6	-	-
Rate of cannibalism	-	0.44	-	-

3. Simulation Results and Discussion

Simply put, the Chess Algorithm (CA) got-shot up and ran under MATLAB, with the simulations into play on a computer under the ages of a Core i5 processor and 16.00 GB RAM. Its primary goal was to see whether CA could optimize the gain parameters of a PI Controller in Load Frequency Control (LFC) for most power systems. Various tests were performed on the architecture's endurance and adaptability: a situation of 10% load perturbation, a case of high load demand, and a case of solar radiation variation-all scenarios of the real world that might be faced by power systems. In optimizing the gains of the PI controller under the above conditions, the CA has indeed shown that it was able to sustain system stability through frequency deviations very effectively.

Testing of the CA-optimized PI controller was done by the ITAE performance index, a perfect index for measuring the response time and accuracy of handling the disturbance by the controller. The checks indicated that the CA algorithm has really done a good job in fine-tuning of the PI controller parameters. Moreover, the algorithm has guaranteed stable frequency control with good load balancing in the power system under varying weather conditions and tough operational scenarios. CA now promises a significant improvement in the overall performance and reliability of the power system control schemes.

3.1. Evaluation of the CA-Optimized Controller in Comparison to Conventional Methods

A load disturbance of 0.1 p.u. affecting both regions enters the system from the third second of testing. It is aimed at investigating how the system behaves when faced with load disturbances and determining how well the controllers perform in frequency stabilization. The controllers are tested against optimal settings for the well-known optimization techniques, with special consideration to the CA in this study.

The controller settings and the corresponding fitness function value obtained using the CA method have been summarized in Table 3. These parameters are the optimally determined PI controller gain values for power output adjustment to returning system frequency to nominal value. The fitness function results are useful for measuring the performance of the optimized controllers in terms of minimizing the errors in the systems and stabilizing under the load disturbances. Thus, the CA optimization is compared with the other optimization techniques.

Table 3. Optimized PI controller parameters from various methods

Parameters	CA-PI (Proposed)	WOA-PI	FA-PI	SSA-PI
K_{p1}	-0.4687	-0.4563	-0.8811	-0.7715
K_{i1}	-0.0923	-0.2254	-0.5765	-0.0483
K_{p2}	-1.9942	-0.8967	-0.7626	-1.0837
K_{i2}	-0.9399	-0.9865	-0.8307	-0.8929

The optimized parameters of the PI controller, shown in Table 3 and obtained by optimization techniques including CA, WOA [62], FA [63], and SSA [35], indicate how crucial the aspects of tuning in power systems are for efficient load frequency control (LFC). The performance of these controllers, as indicated by the fitness function values, can be compared according to the optimization methods employed, thus making it possible to identify which strategy best minimizes error and maintains system stability during perturbations.

Table 4 delineates essential performance measures for assessing the efficacy of modified PI controllers using several methodologies. The table specifically contains the values for undershoot (US) and overshoot (OS). These measurements are vital for comprehending the system's dynamic reaction to load disturbances and are crucial for evaluating the stability and efficacy of the controllers.

Table 4. Performance comparison results for Δf_1 , Δf_2 and ΔP_{tie} with obtained ITAE values

Parameters		CA-PI (Proposed)	WOA-PI	FA-PI	SSA-PI
Δf_1	Undershoot	**-0.15655**	-0.21962	-0.29638	-0.23274
	Overshoot	**0.021149**	0.097358	0.13602	0.060559
Δf_2	Undershoot	**-0.22191**	-0.26681	-0.2757	-0.25713
	Overshoot	**0.046149**	0.10102	0.11731	0.069293
ΔP_{tie}	Undershoot	**-0.02952**	-0.047684	-0.047178	-0.037714
	Overshoot	**0.022811**	0.037722	0.03634	0.032441
ITAE		**2.9104**	4.1211	7.4259	4.9948

The diagram shown in Fig. 3. discusses the flabbergasting comparison in frequency of Area 1 in a dual area power system. The chart delineates time-influenced frequency variations in Area 1, particularly after load disturbance or changes in system conditions. While the x-axis is time measured in seconds, the y-axis is the frequency deviation (Δf_1), quantified by Hertz (Hz), indicating the range of frequency departure from the nominal value.

The system is expected to deviate from its nominal level following disturbance, typically on a much lower or higher level, developing its response to rapid changes in demand in very clear terms. The highest deviation in frequency is assumed to be caused by the greater disturbance to the system; a higher peak represents heavier system reaction. The various lines seen on that graph indicate how the aforementioned PI controllers are tuned according to different approaches, such as Whale Optimization Algorithm (WOA), Firefly Algorithm (FA), Salp Swarm Algorithm (SSA), and Chess

Algorithm (CA). These lines show the performance of each optimization strategy according to how well it minimizes frequency deviations and returns it close to nominal.

These controllers attempt to restore the frequency to its nominal level once it has been disturbed; the time taken to stabilize that frequency would become a significant performance measure. The CA-PI controller is known for its fast recovery with low overshoot and the fastest settling time compared to its competitors, thus depicting high reliability. The performance of all controllers can be evaluated in terms of overshoot, which measures how much the frequency exceeds its nominal value before settling down. The settling time indicates how fast the system returns to its nominal frequency. These parameters are essential for judging the efficiency of each optimization technique in dealing with load changes and maintaining stability in the system.

Fig. 4 shows the frequency variations due to a load disturbance occurring in Area 2 of the power system. The frequency is plotted in deviation from the nominal value against time, where the x-axis denotes time (in seconds) and the y-axis shows frequency deviation in Hertz (Hz). The disturbance effect began approximately at three seconds, which caused an initial deviation of frequency from this nominal value. The controllers of the system are expected to rectify the frequency to nominal, while the graph indicates how the system reacted to this disturbance. The varying frequency is important for checking the efficacy of PI controllers tuned by a variety of algorithms for establishing system stability.

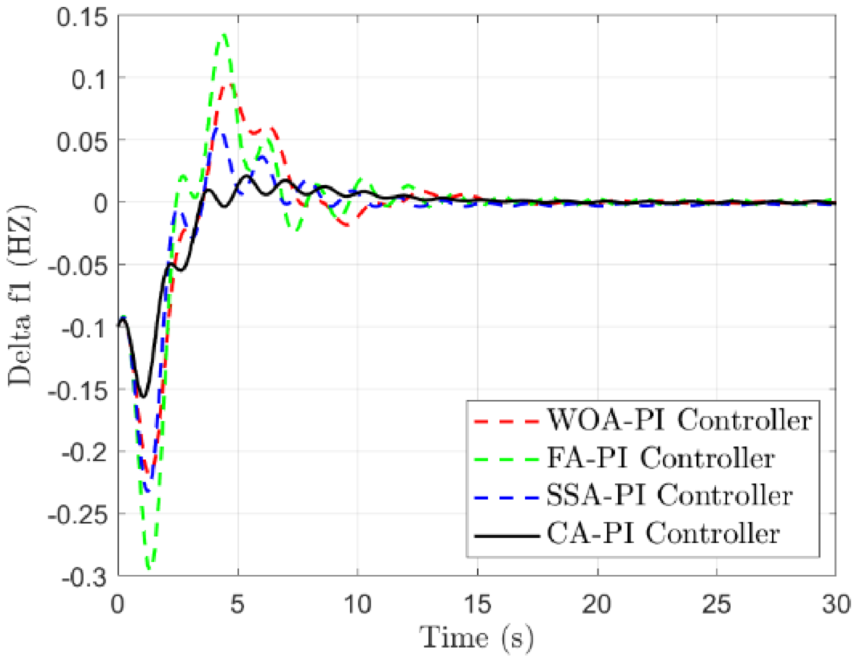

Fig. 4. Frequency deviation in area 1

A line for each optimized PI controller—Whale Optimization Algorithm (WOA), Firefly Algorithm (FA), Salp Swarm Algorithm (SSA), and Chess Algorithm (CA)—has been drawn in the graph. The different graphs describe the system dynamics for the load disturbances due to the respective controllers. The CA-PI controller (black solid line) recovers fastest with little overshoot, thus stabilizing quicker than all others. This shows that the Chess Algorithm-optimized controller is much better at preventing frequency changes and speeding up the system's stabilization. This makes it the best choice for stopping disturbances in Area 2.

Power Fluctuations of Tie Lines with Control Strategies Shown in Fig. 5. This image shows the power variation in the tie line of a dual-area power system, where the PI controllers of each area are tuned using diverse algorithms. The independent variable is time (in seconds), and the dependent variable is tie-line power variation per unit megawatt (pu.MW). The graph displays the system's response to changes, with each line indicating the frequency change caused by various PI controllers.

Four controllers are studied—these controllers are optimized by the Whale Optimization Algorithm (WOA), Firefly Algorithm (FA), Salp Swarm Algorithm (SSA), and Chess Algorithm (CA) with a different optimization technique. Tie line power fluctuations under different control strategies shown in Fig. 6.

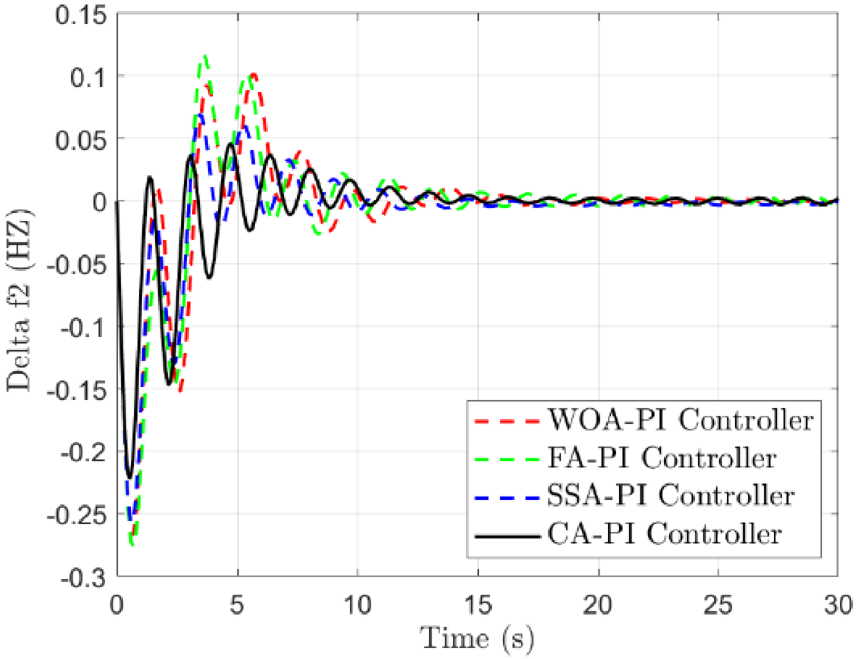

Fig. 5. Frequency deviation in area 2

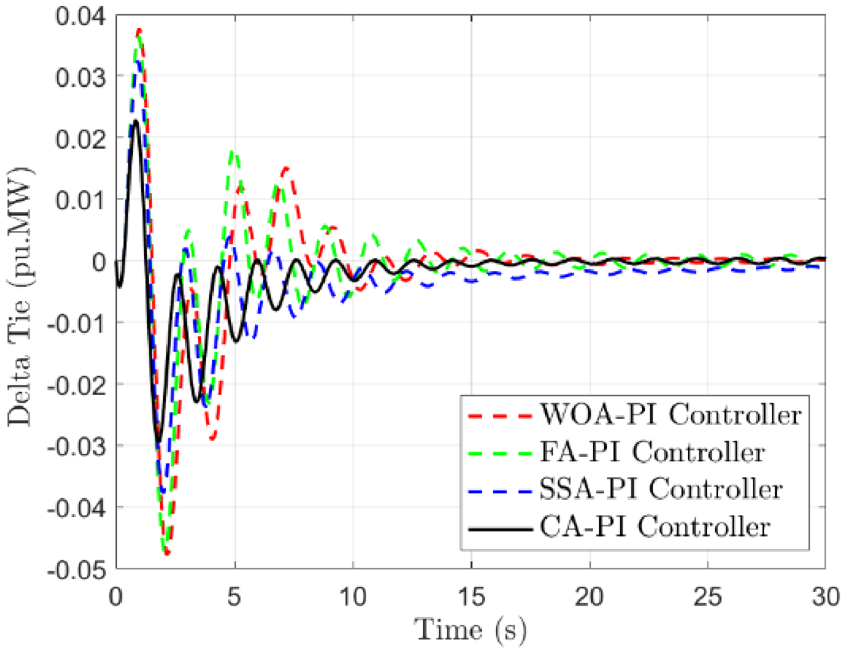

Fig. 6. Tie line power fluctuations under different control strategies

The performance of the controllers can be compared on the basis of how well they could manage tie line power below disturbances. The CA-PI controller (black solid line) has shown supreme performance with lower overshoot and minimum settling time, meaning that tie line power is quickly settled after disturbance. On the other hand, controllers tuned WOA, FA, and SSA optimization techniques to experience major oscillations and prolonged settling times (red dashed, green dash-dotted, and blue dashed lines, respectively). The results show that CA-PI is the best way to control systems because it keeps systems stable even when there are disturbances. This is in contrast to other optimization methods, which make systems more unstable.

4. Conclusions

This paper outlines the creation and systematic assessment of a chess algorithm (CA)-based optimization method for calibrating proportional–integral (PI) controllers in load frequency control (LFC) applications for two-area hybrid photovoltaic–thermal (PV–T) power systems. CA utilizes chess-inspired strategic decision-making mechanisms to enhance the search process, offering improved exploration capabilities and effective evasion of local optima, which are prevalent drawbacks of conventional methods like the Whale Optimization Algorithm (WOA), Firefly Algorithm (FA), and Salp Swarm Algorithm (SSA).

The simulation findings unequivocally indicate that the CA-optimized PI controller attains enhanced performance in managing frequency deviations under diverse operating conditions, such as solar irradiance variations and abrupt load disruptions. The CA technique decreases the integral of time-weighted absolute error (ITAE) by around 29% compared to SSA and markedly reduces overshoot and undershoot values, resulting in quicker settling times compared to the other algorithms assessed. These findings validate the efficacy of the CA as a feasible optimization method for improving frequency regulation in renewable-integrated power grids. Notwithstanding the encouraging outcomes, many limitations of the suggested strategy must be recognized. The research concentrates exclusively on simulation-based analysis, without experimental validation or hardware-in-the-loop (HIL) implementation, both of which are crucial for verifying real-time applicability. Furthermore, although the computational difficulty of CA was not explicitly examined, the chess-inspired method may impose a heightened computing load when the issue size extends to multi-area systems.

Future endeavors will concentrate on expanding the CA-based optimization framework to encompass larger-scale power systems, including multi-area designs with more renewable integration, such as wind, battery storage, and demand response strategies. Additionally, real-time implementation, statistical performance evaluation, and hardware validation will be addressed to improve the practical significance and dependability of the proposed control method.

The suggested CA-based PI controller tuning approach significantly enhances the resilience, stability, and responsiveness of LFC systems in hybrid renewable energy contexts, therefore promoting dependable and sustainable power system operation.

Author Contribution: All authors contributed equally to the main contributor to this paper. All authors read and approved the final paper.

Funding: This research received no external funding

Conflicts of Interest: The authors declare no conflict of interest.

References

[1] Z. Shi, W. Wang, Y. Huang, P. Li, and L. Dong, "Simultaneous optimization of renewable energy and energy storage capacity with the hierarchical control," *CSEE Journal of Power and Energy Systems*, vol. 8, no. 1, pp. 95-104, 2022, https://doi.org/10.17775/CSEEJPES.2019.01470.

[2] H. Guo *et al*., "Synergy-Payoff-Maximization-Based Rechargeable Adaptive Energy-Efficient Dual-Mode Data Gathering Using Renewable Energy Sources," *IEEE Internet of Things Journal*, vol. 11, no. 21, pp. 35292-35305, 2024, https://doi.org/10.1109/JIOT.2024.3434669.

[3] N. M. Haegel and S. R. Kurtz, "Global Progress Toward Renewable Electricity: Tracking the Role of Solar (Version 2)," *IEEE Journal of Photovoltaics*, vol. 12, no. 6, pp. 1265-1272, 2022, https://doi.org/10.1109/JPHOTOV.2022.3206532.

[4] B. Xiao *et al*., “Power Source Flexibility Margin Quantification Method for Multi-Energy Power Systems Based on Blind Number Theory,” *CSEE Journal of Power and Energy Systems*, vol. 9, no. 6, pp. 2321-2331, 2023, https://doi.org/10.17775/CSEEJPES.2020.03730.

[5] D. Yang *et al*., “Adaptive Frequency Droop Feedback Control-Based Power Tracking Operation of a DFIG for Temporary Frequency Regulation,” *IEEE Transactions on Power Systems*, vol. 39, no. 2, pp. 2682-2692, 2024, https://doi.org/10.1109/TPWRS.2023.3277009.

[6] D. T. Trinh, Y. K. Wu, and M. H. Pham, “A Novel Load Frequency Control Strategy for a Modern Power System by Considering State-Space Modeling and Stability Analysis,” *IEEE Access*, vol. 12, pp. 115085-115101, 2024, https://doi.org/10.1109/ACCESS.2024.3445180.

[7] M. Zhang, S. Dong, Z. G. Wu, G. Chen, and X. Guan, “Reliable Event-Triggered Load Frequency Control of Uncertain Multiarea Power Systems With Actuator Failures,” *IEEE Transactions on Automation Science and Engineering*, vol. 20, no. 4, pp. 2516-2526, 2023, https://doi.org/10.1109/TASE.2022.3205176.

[8] B. Wang, Z. Xu, and X. Guan, “Robust Load Frequency Control for Uncertainties Multi-Area Power Systems With Couplings of Systems Dynamics and Reconfigurable Communication Networks,” *IEEE Transactions on Power Systems*, vol. 40, no. 3, pp. 2584-2599, 2025, https://doi.org/10.1109/TPWRS.2024.3453945.

[9] D. Jiao, C. Shao, B. Hu, K. Xie, C. Lin, and Z. Ju, “Age-of-information-aware PI controller for load frequency control,” *Protection and Control of Modern Power Systems*, vol. 8, no. 3, pp. 1-15, 2023, https://doi.org/10.1186/s41601-023-00311-z.

[10] M. S. Iqbal, M. F. A. Limon, M. M. Kabir, M. Z. Hossain, M. F. Jubayer, and M. J. A. Soeb, “A hybrid optimization algorithm based on cascaded (1 + PI)-PI-PID controller for load frequency control in interconnected power systems,” *Results in Engineering*, vol. 24, p. 103624, 2024, https://doi.org/10.1016/j.rineng.2024.103624.

[11] S. Shirali, S. Zolfaghari Moghaddam, and M. Aliasghary, “An interval Type-2 fuzzy Fractional-Order PD-PI controller for frequency stabilization of islanded microgrids optimized with CO algorithm,” *International Journal of Electrical Power & Energy Systems*, vol. 164, p. 110422, 2025, https://doi.org/10.1016/j.ijepes.2024.110422.

[12] T. Pan *et al*., “Strategic integration of residential electricity: An optimisation model for solar energy utilisation and carbon reduction,” *Energy*, vol. 310, p. 133227, 2024, https://doi.org/10.1016/j.energy.2024.133227.

[13] Y. Fu *et al*., “Numerical research on building energy balance and grid stability realization of PV/T-ASHP system through electrical-hydrogen coupled storage technology,” *Energy*, vol. 307, p. 132676, 2024, https://doi.org/10.1016/j.energy.2024.132676.

[14] N. Tak and S. K. Chattopadhyay, “Two-Stage Three-Phase Transformerless Hybrid Multilevel Inverter for Solar PV Application,” *IEEE Transactions on Industrial Electronics*, vol. 71, no. 6, pp. 5386-5398, 2024, https://doi.org/10.1109/TIE.2023.3299027.

[15] X. Shen, H. Shu, Z. Fan, and X. Mo, “Integrated Control Strategy for Electrolytic Aluminum Load Participation in Frequency Modulation,” *IEEE Access*, vol. 9, pp. 56955-56964, 2021, https://doi.org/10.1109/ACCESS.2021.3070864.

[16] X. C. Shangguan, S. Shi, Y. He, and C. K. Zhang, “Optimal Digital Load Frequency Control of Smart Grid Considering Sampling and Time Delay Based on Warm-Up Gray Wolf Algorithm,” *IEEE Transactions on Industrial Informatics*, vol. 21, no. 2, pp. 1773-1782, 2025, https://doi.org/10.1109/TII.2024.3485821.

[17] X. C. Shangguan, C. G. Wei, C. K. Zhang, Y. He, and L. Jiang, “Performance Enhancing Control of Frequency for Future Power Systems With Strong Uncertainties,” *IEEE Transactions on Industrial Informatics*, vol. 20, no. 10, pp. 12439-12449, 2024, https://doi.org/10.1109/TII.2024.3424288.

[18] A. M. A. Soliman, M. B. Eldin, and M. A. Mehanna, “Application of WOA Tuned Type-2 FLC for LFC of Two Area Power System With RFB and Solar Park Considering TCPS in Interline,” *IEEE Access*, vol. 10, pp. 112007-112018, 2022, https://doi.org/10.1109/ACCESS.2022.3215530.

[19] P. Marimuthu, T. Rajesh, N. Rajeswaran, and H. H. Alhelou, “Comparative Performance Analysis of Deregulated Hydrothermal System With Dual Mode Controller and Diverse Source of Generation Employing Imperialistic Competition Algorithm,” *IEEE Access*, vol. 10, pp. 51008-51020, 2022, https://doi.org/10.1109/ACCESS.2022.3172109.

[20] M. A. Zeidan, M. R. Hammad, A. I. Megahed, K. M. AboRas, A. Alkuhayli, and N. Gowtham, “Enhancement of a Hybrid Electric Shipboard Microgrid’s Frequency Stability With Triangulation Topology Aggregation Optimizer-Based 3DOF-PID-TI Controller,” *IEEE Access*, vol. 12, pp. 66625-66645, 2024, https://doi.org/10.1109/ACCESS.2024.3399325.

[21] Z. Qu, W. Younis, X. Liu, A. K. Junejo, S. Z. Almutairi, and P. Wang, “Optimized PID Controller for Load Frequency Control in Multi-Source and Dual-Area Power Systems Using PSO and GA Algorithms,” *IEEE Access*, vol. 12, pp. 186658-186678, 2024, https://doi.org/10.1109/ACCESS.2024.3445165.

[22] G. Dei *et al*., “Improved Squirrel Search Algorithm Driven Cascaded 2DOF-PID-FOI Controller for Load Frequency Control of Renewable Energy Based Hybrid Power System,” *IEEE Access*, vol. 10, pp. 46372-46391, 2022, https://doi.org/10.1109/ACCESS.2022.3169749.

[23] S. Benghazouani, S. Nouh, and A. Zakrani, “Optimizing breast cancer diagnosis: Harnessing the power of nature-inspired metaheuristics for feature selection with soft voting classifiers,” *International Journal of Cognitive Computing in Engineering*, vol. 6, pp. 1-20, 2025, https://doi.org/10.1016/j.ijcce.2024.09.005.

[24] A. Bhetalam and K. A. Naik, “Adaptive maximum power point tracking method for photovoltaic systems using step-size reduction and adapted Salp Swarm Optimization for dynamic conditions,” *Electric Power Systems Research*, vol. 246, p. 111655, 2025, https://doi.org/10.1016/j.epsr.2025.111655.

[25] X. Wei *et al*., “A new intelligent control and advanced global optimization methodology for peak solar energy system performance under challenging shading conditions,” *Applied Energy*, vol. 390, p. 125808, 2025, https://doi.org/10.1016/j.apenergy.2025.125808.

[26] R. Madamaneri and T. Devaraju, “Optimizing Real-Time Scheduling for Post Islanding Energy Management Using African Vulture Optimization Algorithm on Hybrid Microgrids Environment,” *International Journal of Electrical and Electronics Research*, vol. 12, no. 4, pp. 1151-1162, 2024, https://ijeer.forexjournal.co.in/archive/volume-12/ijeer-120405.html.

[27] M. Vaka, R. Walvekar, A. K. Rasheed, M. Khalid, and H. Panchal, “A Review: Emphasizing the Nanofluids Use in PV/T Systems,” *IEEE Access*, vol. 8, pp. 58227-58249, 2020, https://doi.org/10.1109/ACCESS.2019.2950384.

[28] L. Lin, J. Zhang, and S. Shao, “A Variable Switching Frequency Multimode Control Scheme for Single-Phase Grid-Tied Multilevel PV Microinverters,” *IEEE Transactions on Power Electronics*, vol. 38, no. 9, pp. 11543-11555, 2023, https://doi.org/10.1109/TPEL.2023.3274925.

[29] S. Audomsi *et al*., “The development of pid controller by chess algorithm,” *Engineering Access*, vol. 10, no. 1, pp. 46-50, 2024, https://doi.org/10.14456/mijet.2024.6.

[30] T. Buranaaudsawakul, K. Ardhan, S. Audomsi, W. Sa-Ngiamvibool, and R. Dulyala, “Optimal turning of a 2-DOF proportional-integral-derivative controller based on a chess algorithm for load frequency control,” *International Journal of Electrical and Computer Engineering*, vol. 15, no. 1, pp. 146-155, 2025, https://doi.org/10.11591/ijece.v15i1.pp146-155.

[31] S. Xu, R. Shao, B. Cao, and L. Chang, “Single-phase grid-connected PV system with golden section search-based MPPT algorithm,” *Chinese Journal of Electrical Engineering*, vol. 7, no. 4, pp. 25-36, 2021, https://doi.org/10.23919/CJEE.2021.000035.

[32] D. Xu *et al*., “Coupling Analysis of Differential Power Processing-Based PV System and Its Decoupling Implementation of Synchronous MPPT Control,” *IEEE Transactions on Industrial Electronics*, vol. 70, no. 7, pp. 6973-6983, 2023, https://doi.org/10.1109/TIE.2022.3201277.

[33] A. Khazaee, A. Yazdani, H. M. Hesar, and B. Wu, “Efficient MPPT for BLDCM-Driven PV Pumping System Based on Ripple Correlation Control,” *IEEE Transactions on Power Electronics*, vol. 38, no. 7, pp. 8022-8026, 2023, https://doi.org/10.1109/TPEL.2023.3266300.

[34] L. Mamouri, T. Mesbahi, and V. Frick, “MPPT Technique With Improved FOCV Control Applied to a Full Active Rectifier for Low-Voltage Piezoelectric Energy Harvesting,” *IEEE Transactions on Circuits and Systems II: Express Briefs*, vol. 71, no. 2, pp. 532-536, 2024, https://doi.org/10.1109/TCSII.2023.3308956.

[35] S. Ekinci, D. Izci, M. Salman, and H. A. Hilal, “Load Frequency Controller Design of a Two-area Power System via Artificial Rabbits Optimization,” *2024 Advances in Science and Engineering Technology International Conferences (ASET)*, pp. 01-05, 2024, https://doi.org/10.1109/ASET60340.2024.10708668.

[36] P. C. Patra, P. K. Panigrahi, A. Satpathy, and N. Nayak, “Assessing stability in renewable microgrid using a novel-optimized controller for PV-battery based micro grid with OPAL-RT based real-time validation,” *Results in Engineering*, vol. 26, p. 104290, 2025, https://doi.org/10.1016/j.rineng.2025.104290.

[37] T. Baškarad, N. Holjevac, and I. Kuzle, “Photovoltaic System Control for Power System Frequency Support in Case of Cascading Events,” *IEEE Transactions on Sustainable Energy*, vol. 14, no. 2, pp. 1324-1334, 2023, https://doi.org/10.1109/TSTE.2022.3197687.

[38] Q.-Y. Song, U. Zulfiqar, and X. Du, “Finite-frequency model order reduction of linear and bilinear systems via low-rank approximation,” *Journal of Computational and Applied Mathematics*, vol. 457, p. 116287, 2025, https://doi.org/10.1016/j.cam.2024.116287.

[39] P. K. Sorte, K. P. Panda, and G. Panda, “Current Reference Control Based MPPT and Investigation of Power Management Algorithm for Grid-Tied Solar PV-Battery System,” *IEEE Systems Journal*, vol. 16, no. 1, pp. 386-396, 2022, https://doi.org/10.1109/JSYST.2021.3052959.

[40] S. Ekinci, D. Izci, C. Turkeri, A. Smerat, A. E. Ezugwu, and L. Abualigah, “Frequency regulation of two-area thermal and photovoltaic power system via flood algorithm,” *Results in Control and Optimization*, vol. 18, p. 100539, 2025, https://doi.org/10.1016/j.rico.2025.100539.

[41] P. Sreenivasulu and J. Hussain, “Design of cascaded control loops for the implementation of adaptive MPPT control algorithm on doubly fed induction generator based wind energy conversion system,” *Results in Engineering*, vol. 25, p. 104384, 2025, https://doi.org/10.1016/j.rineng.2025.104384.

[42] H. Karimi, A. Siadatan, and A. Rezaei-Zare, “A Hybrid P&O-Fuzzy-Based Maximum Power Point Tracking (MPPT) Algorithm for Photovoltaic Systems under Partial Shading Conditions,” *IEEE Access*, 2025, https://doi.org/10.1109/ACCESS.2025.3533314.

[43] R. Celikel, M. Yilmaz, and A. Gundogdu, “Improved voltage scanning algorithm based MPPT algorithm for PV systems under partial shading conduction,” *Heliyon*, vol. 10, no. 20, p. e39382, 2024, https://doi.org/10.1016/j.heliyon.2024.e39382.

[44] X. Jia, H. Chen, Y. Yang, C. Xu, L. Duanmu, and Z. Wang, “Research on integrative optimization operation of seawater heat pump, photovoltaic, and cross-seasonal heat storage systems,” *Renewable Energy*, vol. 246, p. 122864, 2025, https://doi.org/10.1016/j.renene.2025.122864.

[45] J. M. Mauricio, Á. Rodríguez del Nozal, and A. E. Leon, “A constraint-aware controller for renewable power plant operation under communication delays,” *Electric Power Systems Research*, vol. 246, p. 111635, 2025, https://doi.org/10.1016/j.epsr.2025.111635.

[46] Y. Pedari, C. Freiheit, D. M. Anand, and H. R. Ossareh, “Parametrized Maximal Admissible Sets With Application to Constraint Management of Systems With Slowly Varying Parameters,” *Journal of Dynamic Systems, Measurement and Control*, vol. 147, no. 4, p. 041007, 2025, https://doi.org/10.1115/1.4067513.

[47] S. Santra, S. Mondal, and M. De, “Enhanced frequency control of a hybrid microgrid integrated with EV aggregator using [FOI-(PDN+1)] controller optimized by osprey optimization algorithm,” *Engineering Research Express*, vol. 7, no. 2, p. 025303, 2025, https://doi.org/10.1088/2631-8695/adc53d.

[48] M. I. Shahzad, M. M. Gulzar, S. Habib, M. Shafiullah, A. Shahzad, and M. Khalid, “Advanced frequency stabilization framework for multi-area renewable energy grids with EV aggregator support: A multi-stage control perspective,” *Sustainable Computing: Informatics and Systems*, vol. 46, p. 101120, 2025, https://doi.org/10.1016/j.suscom.2025.101120.

[49] S. H. Jakobsen, X. Bombois, S. S. Acevedo, H. Haugdal, and S. D'Arco, “A data driven approach using local measurements to locate turbine governors causing forced oscillations,” *International Journal of Electrical Power and Energy Systems*, vol. 168, p. 110633, 2025, https://doi.org/10.1016/j.ijepes.2025.110633.

[50] C. D. Vournas and A. Zaharakis, “Hydro turbine transfer functions with hydraulic coupling,” *IEEE Transactions on Energy Conversion*, vol. 8, no. 3, pp. 527-532, 1993, https://doi.org/10.1109/60.257069.

[51] N. Alqahtani, “A Novel Privacy Framework for Satellite Images Based on Theory of Chaos and Chess Pieces Castle and King,” *IEEE Access*, vol. 13, pp. 40503-40519, 2025, https://doi.org/10.1109/ACCESS.2025.3541833.

[52] M. Fadaki and A. Asadikia, “Augmenting Monte Carlo Tree Search for managing service level agreements,” *International Journal of Production Economics*, vol. 271, p. 109206, 2024, https://doi.org/10.1016/j.ijpe.2024.109206.

[53] H. Itoh, Y. Kihara, H. Fukumoto, and H. Wakuya, “Using Particle Representation of Beliefs in an Alphazero-Based Reinforcement Learning Algorithm for Partially Observable Environments,” *ICIC Express Letters*, vol. 18, no. 3, pp. 219-227, 2024, https://doi.org/10.24507/icicel.18.03.219.

[54] F. Jubair, A. Abu Salem, Y. Assaf, and K. A. Darabkh, “GoFish: A customizable open-source chess engine in Go,” *Expert Systems with Applications*, vol. 250, p. 123855, 2024, https://doi.org/10.1016/j.eswa.2024.123855.

[55] Z. Gao, M. Han, S. Liu, A. Li, and D. Mu, “High utility itemsets mining based on hybrid harris hawk optimization and beluga whale optimization algorithms,” *Journal of Intelligent and Fuzzy Systems*, vol. 46, no. 4, pp. 7567-7602, 2024, https://doi.org/10.3233/JIFS-236793.

[56] S. P. Yadav, M. Jindal, P. Rani, V. H. C. de Albuquerque, C. dos Santos Nascimento, and M. Kumar, “An improved deep learning-based optimal object detection system from images,” *Multimedia Tools and Applications*, vol. 83, no. 10, pp. 30045-30072, 2024, https://doi.org/10.1007/s11042-023-16736-5.

[57] S. Audomsi, S. Wattana, N. Uthathip, and W. Sa-ngiamvibool, “Development and Design of an Optimal Fuzzy Logic Two Degrees of Freedom-Proportional Integral Derivative Controller for a Two-Area Power System Using the Bee Algorithm,” *Energies*, vol. 18, no. 4, p. 915, 2025, https://doi.org/10.3390/en18040915.

[58] J. W. Simpson-Porco, “On Area Control Errors, Area Injection Errors, and Textbook Automatic Generation Control,” *IEEE Transactions on Power Systems*, vol. 36, no. 1, pp. 557-560, 2021, https://doi.org/10.1109/TPWRS.2020.3029418.

[59] M. I. Alam Shithil *et al.*, “Performance enhancement of a vented quarter-circular solar thermal collector using proportional, proportional-integral, and proportional-integral-derivative controllers,” *Applied Thermal Engineering*, vol. 269, p. 126127, 2025, https://doi.org/10.1016/j.applthermaleng.2025.126127.

[60] S. Ekinci *et al.*, “A novel pressure control method for nonlinear shell-and-tube steam condenser system via electric eel foraging optimizer,” *Scientific Reports*, vol. 15, no. 1, p. 7550, 2025, https://doi.org/10.1038/s41598-025-92576-7.

[61] C. Andic, S. Ozumcan, M. Varan, and A. Ozturk, “A Novel Sea Horse Optimizer Based Load Frequency Controller for Two-Area Power System with PV and Thermal Units,” *International Journal of Robotics and Control Systems*, vol. 4, no. 2, pp. 606-627, 2024, https://doi.org/10.31763/ijrcs.v4i2.1341.

[62] O. Can and M. S. Ayas, “Gorilla troops optimization-based load frequency control in PV-thermal power system,” *Neural Computing and Applications*, vol. 36, no. 8, pp. 4179-4193, 2024, https://doi.org/10.1007/s00521-023-09273-7.

[63] S. M. Abd-Elazim and E. S. Ali, “Load frequency controller design of a two-area system composing of PV grid and thermal generator via firefly algorithm,” *Neural Computing and Applications*, vol. 30, no. 2, pp. 607-616, 2018, https://doi.org/10.1007/s00521-016-2668-y.